



HAL
open science

Dynamic parameterization of soil surface characteristics for hydrological models in agricultural catchments

Thomas Grangeon, Rosalie Vandromme, Lai Ting Pak, Philippe Martin,
Olivier Cerdan, Jean-Baptiste Richet, Olivier Evrard, Véronique Souchère,
Anne-Véronique Auzet, Bruno Ludwig, et al.

► To cite this version:

Thomas Grangeon, Rosalie Vandromme, Lai Ting Pak, Philippe Martin, Olivier Cerdan, et al.. Dynamic parameterization of soil surface characteristics for hydrological models in agricultural catchments. CATENA, 2022, 214, pp.106257. 10.1016/j.catena.2022.106257 . hal-03645062

HAL Id: hal-03645062

<https://hal.inrae.fr/hal-03645062>

Submitted on 19 Apr 2022

HAL is a multi-disciplinary open access archive for the deposit and dissemination of scientific research documents, whether they are published or not. The documents may come from teaching and research institutions in France or abroad, or from public or private research centers.

L'archive ouverte pluridisciplinaire **HAL**, est destinée au dépôt et à la diffusion de documents scientifiques de niveau recherche, publiés ou non, émanant des établissements d'enseignement et de recherche français ou étrangers, des laboratoires publics ou privés.

Copyright

1 Dynamic parameterization of soil surface characteristics for
2 hydrological models in agricultural catchments

3 Thomas Grangeon^(a), Rosalie Vandromme^(a), Lai Ting Pak^{(b),(c)}, Philippe Martin^(d), Olivier Cerdan^(a), Jean-
4 Baptiste Richet^(c), Olivier Evrard^(e), Véronique Souchère^(f), Anne-Véronique Auzet^(g), Bruno Ludwig^(h),
5 Jean-François Ouvry^(c)

6 (a) BRGM, F-45060, 45060 Orléans, France

7 (b) UPR HortSys, Cirad, F-97285 Le Lamentin, Martinique, France

8 (c) Association de recherche sur le Ruissellement, l'Erosion et l'Aménagement du Sol (AREAS), 2 Avenue Foch,
9 76460 Saint-Valéry-en-Caux

10 (d) Université Paris-Saclay, INRAE, AgroParisTech, UMR SADAPT, 75005, Paris, France

11 (e) Laboratoire des Sciences du Climat et de l'Environnement (LSCE-IPSL), UMR 8212 (CEA/CNRS/UVSQ),
12 Université Paris-Saclay, Gif-sur-Yvette, France

13 (f) UMR SADAPT, INRAE, AgroParisTech, Université Paris-Saclay, Avenue Lucien Brétignières, 78850 Thiverval-
14 Grignon, France

15 (g) Université de Strasbourg, ITES UMR 7063, Strasbourg F-67084, France

16 (h) LIOSE, 71 Rue de Crécy, 02000 Laon

17 * Corresponding author: t.grangeon@brgm.fr

18 Abstract

19 The detrimental impacts of surface runoff and soil erosion, particularly in cultivated areas, call for the
20 use of distributed runoff and soil erosion models with a view to supporting adapted catchment
21 management strategies. However, runoff model parameterization remains challenging in agricultural
22 catchments due to the high spatial and seasonal variability of soil properties. Data acquisition is
23 demanding and may not always be feasible. Therefore, model parameterization in such environments
24 have been the subject of numerous research efforts. The combined analysis of land use management
25 and soil surface state was proposed in literature to address this issue and demonstrated its potential
26 for runoff analysis and modelling. However, these research findings were related to specific rainfall
27 sequences and/or soil surface state. In this study, existing knowledge on soil surface state and its
28 application to runoff model parameterization were synthesized and included in an easy-to-use
29 parameterization software (PREMACHE), providing a framework for modelers lacking of means and/or
30 data for modelling complex agricultural catchments.

31 To develop and evaluate the software, a dataset was acquired over 9 years on more than 110 plots in
32 a 1045 ha agricultural catchment, including crop types, soil surface state, rainfall and runoff time series.
33 Soil surface state dynamics was modeled based on crop types and daily rainfall. It was evaluated in the
34 experimental catchment and validated in a nearby catchment. Soil hydrodynamic properties (e.g.
35 infiltration capacity) were deduced from this framework and literature data at a daily time step, for
36 each plots. Moreover, runoff events were measured when the modeled infiltration capacity was low,
37 indicating that the parametrization adequately captured its temporal dynamics. The software
38 developed in this study, as well as setup values deduced from the monitoring campaigns are provided
39 with the manuscript for application in other ungauged catchments and explore their impact on
40 agricultural catchment hydrological dynamics.

41 **Keywords:** Crops, Soil properties, Runoff, Agricultural catchment, Model parameterization, Soil
42 infiltration capacity, Tillage operations

43 Highlights

- 44 • Parameterization of runoff models is challenging in agricultural catchments
- 45 • Knowledge on using soil surface state for model parameterization was synthesized
- 46 • A comprehensive field survey was performed on a 1045 ha agricultural catchment
- 47 • A simple framework for soil surface state is proposed and evaluated for common crops
- 48 • A software is provided to derive runoff model inputs from rainfall and crop types

49

50 1. Introduction

51 Soil erosion may generate numerous detrimental environmental impacts, including the on-site loss of
52 fertile soil and the off-site triggering of muddy floods, resulting in the degradation of the road network
53 and housing (Boardman et al., 1994; Boardman, 2020). Downstream, the increased fine particles load
54 to rivers is detrimental to aquatic environment (Owens et al., 2005). Muddy floods are regularly
55 observed in the European loess belt (Evrard et al., 2007; Boardman, 2010; Evrard et al., 2010), where
56 the soil erodibility is high and agriculture provides the dominant land use (Cerdan et al., 2004). Models
57 are therefore needed to design effective mitigation strategies to reduce erosion and muddy flood
58 impacts. However, the adequate modelling of runoff and erosion in agricultural catchments requires a
59 spatially-distributed description of the highly variable hydrodynamic properties of soil surface
60 (Gascuel-Oudoux et al., 2011; Gumiere et al., 2011). Indeed, soil hydrodynamic properties such as
61 infiltration capacities can exhibit large spatial variations, resulting from crop allocation decisions and
62 management operations (Shore et al., 2013), as well as large temporal variations because of crusting
63 and roughness evolution throughout the year.

64 Different modelling approaches have been applied to agricultural catchments, such as the spatially
65 distributed LISEM (De Roo et al., 1996) or STREAM (Cerdan et al., 2002a; Evrard et al., 2009) models,
66 or the widely used lumped SWAT/SWAT+ model (Arnold et al., 1998; Bieger et al., 2017). In runoff and
67 erosion models, the parameterization used to calculate the partition of rainfall between runoff and
68 infiltration is critical and, as such, questioned (Qi et al., 2020). The curve number approach (Ponce &
69 Hawkins, 1996) has been used in several models, including SWAT. This approach was criticized as being
70 an empirical formulation of runoff, which may result in an incorrect representation of hydrology (Garen
71 and Moore, 2005; Hawkins, 2014). However, using curve number adaptations following methods such
72 as that proposed by Martin et al. (2009) could provide an adequate formulation of infiltration and
73 runoff calculation in agricultural environments. Finding alternative approaches to include the seasonal
74 variability associated with the crop growth and management in these modelling approaches conducted

75 at the catchment scale remains a topic of wide scientific interest (Nkwasa et al., 2020; Msigwa et al.,
76 *under review*).

77 Another common approach included in hydrological models to describe runoff dynamics is the use of
78 infiltration capacity maps, which can be used to calculate the runoff and infiltration partition using e.g.
79 the Green-Ampt formula (King et al., 1999). Measuring infiltration capacity on multiple plots during
80 the entire crop growth and harvest period and during intercrops, which have a strong impact on runoff
81 and erosion (Cerdan et al., 2002b), would however be time- and labor-consuming and limit their
82 widespread application. To overcome this challenge, many experiments such as those referenced in
83 Cerdan et al. (2002a) were performed to monitor runoff from the plot to the catchment scales in both
84 agricultural and natural environments. These experiments demonstrated that soil surface state,
85 particularly soil crusting, but also soil roughness and crop cover mainly controlled runoff and erosion
86 dynamics (e.g. Duley, 1939; Auzet et al., 1993), and could be used to infer soil hydrodynamic
87 properties. Several classifications of the soil surface state have been developed (e.g. Boiffin et al.,
88 1988) and used to understand runoff and erosion processes in various environments such as West and
89 Sub-Saharan Africa (Casenave and Valentin, 1992; Valentin, 1991), Australia (Moss and Watson, 1991;
90 Foley et al., 1991), Israel (Eldridge et al., 2000), USA (Baumhardt et al., 1991; Le Bissonnais and Singer,
91 1992), Iran (Eghbal et al., 1996) and Northern Europe (Auzet et al., 1995; Van Dijk and Kwaad, 1996;
92 Le Bissonnais et al., 2005; Evrard et al., 2008). Numerous runoff and infiltration equations have been
93 elaborated using these parameters (Seginer and Morin, 1969; Brakensiek and Rawls, 1983; Assouline
94 and Mualem, 1996). Models using this approach demonstrated their ability to predict runoff and
95 erosion in agricultural fields in various contexts on loess soils (e.g. in France and Belgium), suggesting
96 that they adequately captured the main runoff dynamics drivers, as well as their temporal variations
97 (Evrard et al., 2009). Most importantly, these studies provided a methodology to create soil
98 hydrodynamic properties maps that may be used by physically based models (e.g. De Roo and
99 Riezebos, 1992), and to account for their spatial and temporal variability. Soil surface state classes can
100 also be directly be used to incorporate infiltration, imbibition (reflecting pre-ponding rainfall),

101 Manning's coefficient (Cerdan et al., 2002a), but also erosive parameters such as the potential
102 suspended sediment concentration (Cerdan et al., 2002b) in expert based runoff and soil erosion
103 models (Bartman et al., 2020).

104 However, even if monitoring soil surface state requires limited efforts and could be used to create
105 adequate runoff model inputs, such monitoring strategies are time-consuming, which may not always
106 be feasible (e.g. in remote catchments locations, for time and/or money constraints). The literature is
107 therefore lacking means to account for the potentially high spatial and temporal variability of soil
108 surface properties and to represent runoff dynamics in agricultural catchments.

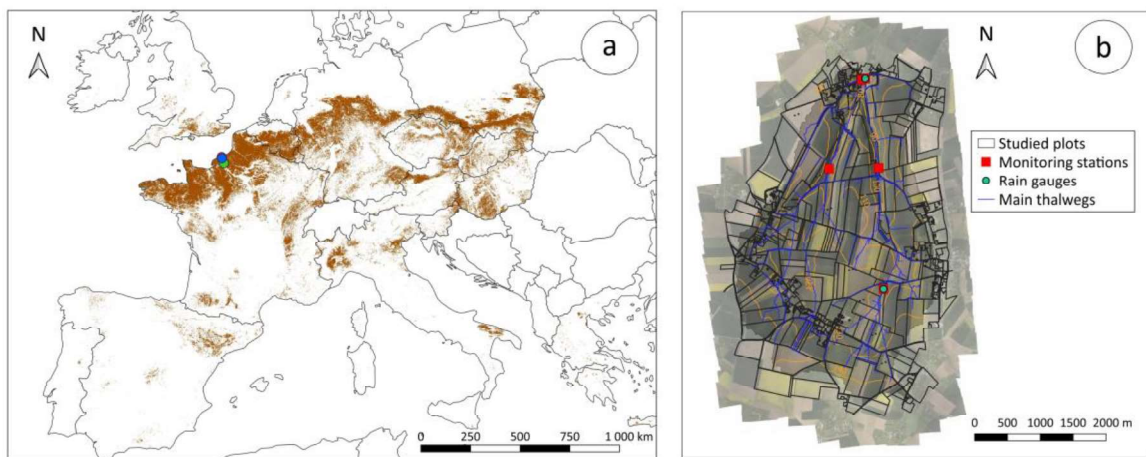
109 Accordingly, the goal of our research was to develop and evaluate a parametrization software
110 producing runoff and erosion model inputs: the PREMACHE (Parameterization of Runoff and Erosion
111 Models in Agricultural Catchments) software. It provides users with an easy approach when using
112 models to address the complex hydro-sedimentary behavior of agricultural catchments. This approach
113 is based on the use of soil surface state as proxies of soil hydrodynamic properties the validity of which
114 was demonstrated the literature. A simple parameterization of soil surface state dynamics over
115 common crop types is proposed, and evaluated in an agricultural catchment located in the European
116 loess belt. Soil hydrodynamic properties, such as infiltration capacity, were deduced from the modeled
117 soil surface state and literature data review. It was then used to analyze the impacts of the soil
118 properties spatial and temporal heterogeneities on the catchment dynamics. Finally, the toolbox used
119 to create runoff model inputs is provided with setup values along with the manuscript to support
120 models parameterization for ungauged agricultural catchments.

121 2. Methods

122 2.1. Study area

123 The monitoring campaigns were performed in the Bourville catchment, located in Upper Normandy,
124 France (Figure 1a), within the European loess belt, defined as the "Silt" and "Silt-loam" texture in the
125 USDA classification applied to the dataset proposed by Ballabio et al. (2016). This site is a 1045 ha

126 catchment which was mainly covered, during the monitoring period of almost 9 years (September, 26th
127 2007 - May, 31th 2016) with cropland (72%), grassland (18%), urban (6%) and forested areas (4%). The
128 main crops were, relative to the total crops area, wheat (42%), flax (16%), rapeseed (13%), sugar beet
129 (7%), winter barley (7%), potatoes (6%) and maize (6%).



130
131 Figure 1: a) Location of the study area in Europe. The Bourville (blue) and nearby Blosseville (red) and
132 Austreberthe (green) catchments are located within the European loess belt (brown areas). The experimental
133 setup of the Bourville catchment is presented in subfigure b).

134 The catchment is mainly covered with Neoluvisol and Brunisol soils. According to the USDA soil textural
135 classification, soils are referred to as silts and silt loams, associated with a low structural stability. These
136 soils developed on well-drained thick soils, overlying karstic geological formation. Silt and silt loam
137 corresponded to more than 9% of the surface area of the European soil texture dataset proposed by
138 Ballabio et al. (2016), indicating that the studied catchment soils are representative of cultivated soils
139 across the continent. These soil types have been described as sensitive to surface crusting, affecting
140 the soil's hydrodynamic properties. Indeed, an increase in crusting results in a decrease of the
141 infiltration capacity (Boiffin et al., 1988; Le Bissonnais et al., 1998). Additional data were also collected
142 from literature for the nearby Blosseville and Austreberthe catchments (section 2.2.2): they were
143 located 10 km north and 30 km south of the Bourville catchment, respectively. Both sites are covered
144 with silt loam soils developed on loess Quaternary deposits. These catchments included a large

145 proportion of cultivated areas: more than 90% for the Blossenville catchment (90 ha) and 60% for the
 146 Autreberthe catchment (215 km²). Additional details on these catchments can be found in Cerdan et
 147 al. (2002a) and Delmas et al. (2012), respectively.

148 2.2. Field measurements

149 2.2.1. Crop type and soil surface state monitoring

150 On average during the monitoring period, 110 plots were surveyed in the Bourville catchment. The
 151 associated crops types, seeding, harvesting and tillage operations (e.g. ploughing) dates were
 152 determined through farmers' interviews and field observations. Crusting stage, crop cover and
 153 roughness were also monitored for 19 different crops following the procedure described in Boiffin et
 154 al. (1988) and Ludwig (1992). Two micro-plots (50 cm x 35 cm) were delimited in each plot,
 155 photographs were taken and observations were performed on the field to evaluate crop cover and
 156 surface roughness. The specific procedures described in Bresson and Boiffin (1990) were used to define
 157 the crusting stage. These procedures are based on morphological descriptions of clods size and shape,
 158 and estimation of inter-clods patches of continuous areas where interstices disappeared. These
 159 observations were performed at different periods to capture plant growth and crusting development.
 160 The corresponding crops and monitoring classes were reported in Table 1.

Crop cover index		Crusting		Roughness		Monitored crop types
C1	0 – 20 %	F0	Fragmentary	R0	0 - 1 cm	Wheat x 4 (N=42)
			stage			Flax x 2 (N=24)
C2	21 – 60 %	F1	Structural	R1	1 - 2 cm	Rapeseed x 2 (N=20)
			stage			Sugar beet x 2 (N=22)
C3	61 – 100 %	F12	Intermediate	R2	2 - 5 cm	Potatoes x 2 (N=18)
			crusting			Maize x 2 (N=16)
		F2	Sedimentary	R3	5 - 10 cm	Peas x 2 (N=14)
			crust			Intercrops x 3 (N=22)

161

Table 1: Soil surface state, associated nomenclature and crop types monitored for their soil surface state. The
162 number of monitored plots and total observation numbers (in parenthesis, including the two locations and the
163 temporal observations) are indicated in the last column.

164 The monitored crops represented the most common plants cultivated in the catchment (section 2.1).
165 Several plots were monitored to include a variety of crop rotations type. For each monitored plot, the
166 crop cover, crusting and roughness level were assessed for the two micro-plots and during various
167 measurement periods to capture the entire growing cycle. Measurements were performed between
168 four and seven times (on average five times) over the monitoring period, depending on the crop
169 growing duration. In total, 176 observations were used for this study. Depending on the crop growing
170 cycle duration, each crop type was monitored for a period comprised between 51 and 202 days (mean
171 126 days).

172 2.2.2. Additional soil surface state data

173 To increase the database robustness, the 204 observations on plots cultivated with wheat presented
174 by Delmas et al. (2012) were used in the current research to generate the parameterization proposed
175 in section 3.2 and 3.3. In the current research, results will be presented only for the main winter (i.e.
176 wheat) and spring (i.e. flax) crop types observed in the Bourville catchment. Additional figures, showing
177 parameterization performance for the other monitored crops, can be found in supplementary material
178 for evaluation over a variety of crop types. Moreover, the parameterization was validated on
179 measurements performed in the Blossenville catchment in section 3.4. The latter included rainfall and
180 soil surface state observations on 20 plots at 5 to 6 dates along the entire crop cycle, corresponding to
181 an additional 109 observations over an additional year. Results are also presented in supplementary
182 material. In this study, 489 observations were used including 380 records for parameterization and 109
183 for validation. This compilation relied on observations made across three different catchments and
184 contrasted monitoring periods, corresponded to three years of monitored data. It is therefore

185 expected that this compilation would produce results that can be extrapolated to other catchments,
186 as it included various rainfall depths, intensity, kinetic energy, as well as variations in temperatures
187 and soil textures.

188 2.3. Monitoring stations and data processing

189 Rainfall and water discharge were measured in the Bourville catchment. Measurement of water
190 discharge was contemporary to rainfall period. Rainfall was monitored with automatic rain gauges at
191 a 6-minutes time step (Précis Mécanique 3029) from September 2007 to May 2016. Mean annual
192 rainfall was ranging from 629 mm to 974 mm, with a mean of 769 mm over the monitoring period. The
193 mean long-term (1981-2010) annual rainfall recorded at the nearby Le Havre station is 790 mm with a
194 mean monthly rainfall ranged from 52 mm (February) to 89 mm (December). The monitored rainfall is
195 therefore representing average conditions, including both dry and wet years.

196 Water discharge was measured at four locations in the catchments, including nested measurements
197 in sub-catchments. In this study, we only used data from the station located at the catchment outlet.
198 Discharge was measured using a calibrated flume, using water height probes (INW PT12) measuring
199 water height at a high frequency, and recorded using a ISCO 2105G data logger. The monitoring
200 frequency ranged from one to six minutes, depending on the monitoring period. Gauging was
201 performed using a velocimeter (Valport 801 flat) or the salt dilution method, depending on the
202 discharge range. Gauging was combined with water height levels to establish rating curves (Richet et
203 al., 2021), resulting in high-frequency discharge monitoring at each station. The rating curve fitted well
204 with the 13 measurements; the determination coefficient was 0.99 at the catchment outlet. Measured
205 discharge ranged from $0.04 \text{ m}^3 \cdot \text{s}^{-1}$ to $2.7 \text{ m}^3 \cdot \text{s}^{-1}$. 95.7% of the values recorded during the monitoring
206 period were included in this range, indicating its representativity. Field observations lead since 1994
207 did not revealed any spring in the catchment, and it had no watercourses, only ditches (Richet et al.,
208 2021). Therefore, the measured discharge results only from runoff.

209 Individual rainfall events were defined from the rainfall time series measured at a 6-minutes time step.
210 One individual event was defined as more than 1 mm of rain, separated from the following event by
211 at least 3 hours without rainfall. Rainfall depth, duration and intensity were then calculated for each
212 rainfall event. Individual runoff events were defined from the discharge time series as events with a
213 peak discharge higher than $0.03 \text{ m}^3 \cdot \text{s}^{-1}$ and a total volume higher than 0.01 mm. Runoff volume,
214 duration, peak discharge were calculated for analyzing the catchment hydrological dynamics
215 (performed in Richet et al., 2021). This procedure was adapted from the methodology proposed by
216 Grangeon et al. (2021). The parametrization developed in this study made use of rainfall depth and
217 intensity during the rainfall events, as well as rainfall depth occurring prior to runoff events, considered
218 a proxy of soil moisture (Cerdan et al., 2002).

219 The Mood test was used at the 5% level of significance to test for median differences between groups
220 in rainfall and runoff distributions. To assess the parameterization performance, the Kruskal-Wallis test
221 was used at the 5% level of significance.

222 2.4. PREMACHE framework description

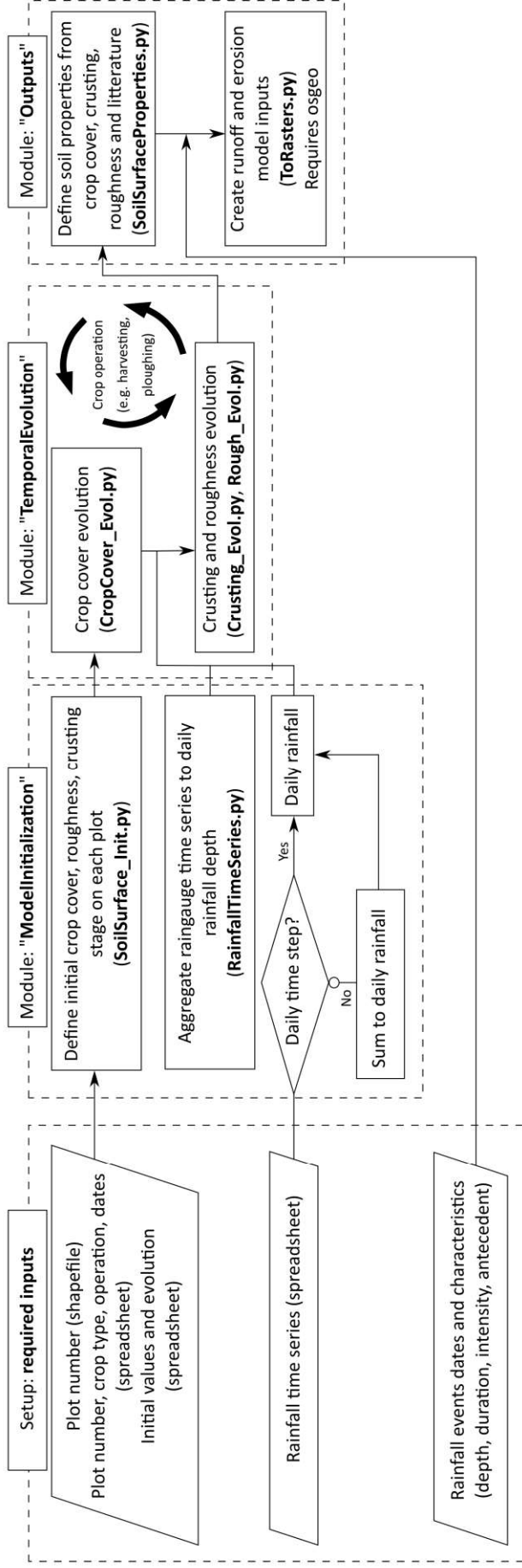
223 2.4.1. Model summary

224 The objective of the PREMACHE software was to generate soil hydrodynamic property maps that can
225 be readily used as runoff and erosion models inputs. The following model inputs can be created at a
226 daily time step: infiltration capacity, imbibition and Manning's n coefficient. Additional variables
227 related to erosion modelling are also provided (sheet erosion concentration and soil erodibility), based
228 on the data proposed by Cerdan et al. (2002b). However, in this study, results will focus on infiltration
229 capacity, as it is one of the main runoff model requirements.

230 To create a spatial distribution of these parameters (maps), the soil surface state is modeled by
231 PREMACHE at a daily time step, on each plot across the catchment. For each plot, PREMACHE initialized
232 the crop cover, crusting and roughness based on empirical data depending on the crop type, previous
233 shallow tillage operations and potential chemical crop destruction. Crop cover was then modeled to

234 increase with time over the modeled period, depending on the crop type. Empirical data from the
235 current study was provided as default values for different crop type. PREMACHE then combined the
236 crop cover with rainfall records to model soil crusting and roughness evolution. Crop operations are
237 considered, as they may modify both crop cover (e.g. harvesting) and surface crusting and roughness
238 through tillage operations (e.g. ploughing).

239 Finally, conversion of soil surface states into hydrodynamic properties was performed using the
240 procedure described in the STREAM model (Cerdan et al., 2002a). The Manning coefficient was derived
241 from the experimental data proposed for various crop types by Gilley et al. (1991) and Morgan (2005).
242 These values can also be modified on the corresponding input spreadsheet. The software functioning
243 is summarized in Figure 2.



245 Figure 2 : Flowchart of the PREMACHE software and associated individual scripts.

246 Values acquired in the current study are provided with the toolbox and may be used as default values
247 in similar although unmonitored catchments. Otherwise, values can be modified in the spreadsheets
248 to reflect changes in soil properties for instance.

249 The GIS files were processed using QGIS (QGIS, 2022; V.3.10 - A Coruña). The toolbox was developed
250 as a sequence of scripts using Python V.3.8.5 and is available at <https://github.com/BRGM/premache>

251 2.4.2. Required inputs

252 The required inputs are:

- 253 • A raster providing the expected resolution and extent, such as the Digital Elevation Model
254 (DEM).
- 255 • A shapefile corresponding to the catchment plots. Each plot should be associated with a plot
256 (arbitrary) number. As the plot sizes and locations may change over time, multiple shapefiles
257 can be used to reflect the land use temporal evolution. Monitored data, national databases
258 providing annual maps or statistics can be used to fill in this spreadsheet.
- 259 • A spreadsheet file indicating the land use (including crop type and farming operations) at each
260 measurement period, with the associated plot numbers.
- 261 • A two-column file including the rain gauge records. Rainfall records should be provided with a
262 daily time step. If a higher resolution is available, the toolbox can be used to decrease the
263 resolution to a daily time step in order to avoid high frequency variations while conserving an
264 adequate temporal resolution regarding the timescales involved in the control of soil surface
265 state evolution.
- 266 • A file including rainfall events characteristics for which runoff model inputs will be generated.
267 Users should provide one or multiple dates of interest in a specific file, corresponding to
268 rainfall events that should be modeled, with their associated characteristics: rainfall depth,
269 duration maximum intensity and rainfall depth over the past two days before the rainfall
270 event.

- 271 • Three different tables describing the evolution of:
- 272 ○ Crop cover increase as a function of time and crop cover decrease dynamics under
- 273 different farming operation types. In the current research, ploughing and chemical
- 274 destruction were considered separately, as described below (section 3.2).
- 275 ○ Surface roughness and crusting as a function of both cumulative rainfall and crop cover
- 276 (section 3.3).

277 2.4.3. Limitations and adaptations

278 In the toolbox, crops are assumed to grow independently from rainfall and temperature. Our dataset,

279 and the corresponding parameterization, should therefore need additional calibration for catchments

280 undergoing severe dry or wet periods. We are also aware that process-based approaches were

281 proposed in the literature (Peñuela et al., 2018; Boas et al., 2021), for instance to model crop growing

282 at various scales. However, the goal of the current research was to provide measurement data and a

283 simple parameterization to obtain reliable estimates of soil surface evolution, based on limited input

284 requirements. Moreover, the software made use of simple spreadsheets; values can therefore be

285 easily modified according to the scientists' knowledge, or using dedicated measurements or more

286 detailed crop growing modelling.

287 This toolbox was developed for agricultural fields on soils prone to surface crusting, and may therefore

288 need additional calibration to describe soil surface evolution in catchment located in a different

289 climate context and on different soils (i.e. loess-derived silt-sized soils) than those typically found in

290 the European loess belt, for instance following the methodology proposed in Ludwig (1992) or Evrard

291 et al. (2009). While it should help modelers in representing soils hydrodynamics properties, they

292 should adapt the proposed values depending on the dominant processes occurring in the modeled

293 catchment. It should also be noted that this approach was successfully adapted by Gascuel-Odoux et

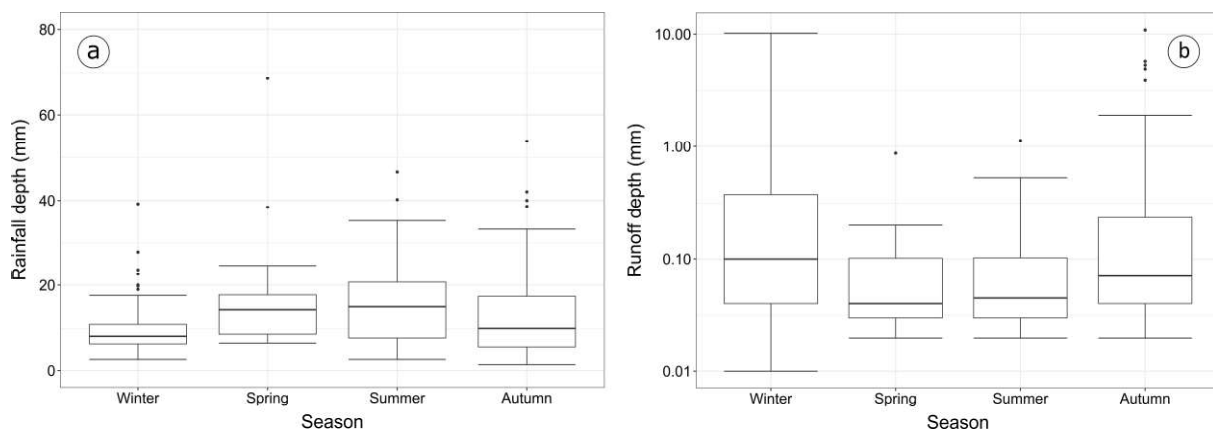
294 al. (2009) and Evrard et al. (2009) for catchments of Western France, Southern France and Belgium,

295 suggesting that it may be implemented in catchments located in other regions.

296 3. Results and discussion

297 3.1. Rainfall and crop types variations over the monitoring period

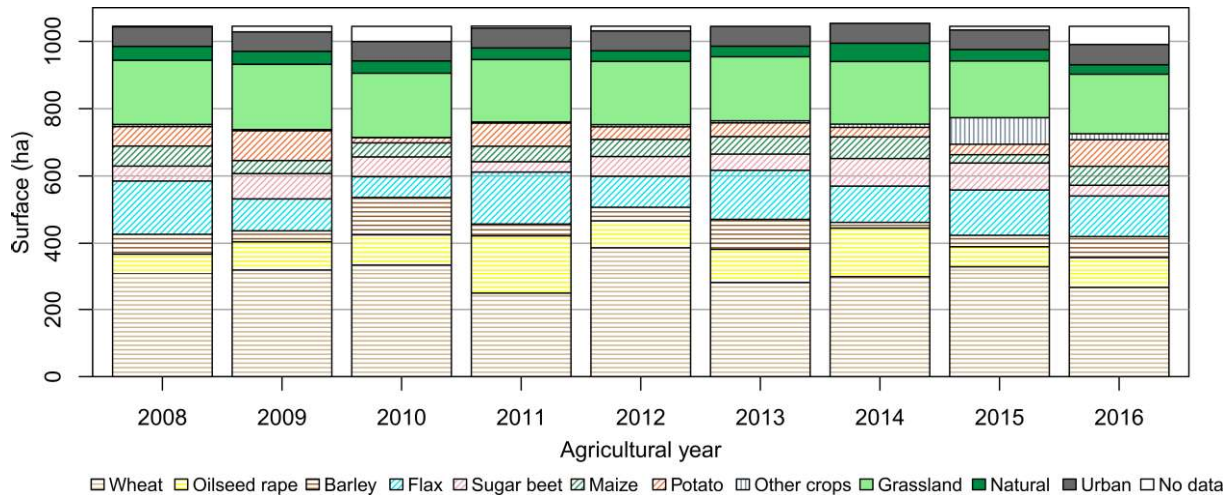
298 During the monitoring period, 227 runoff events were recorded. Among them, 40 (18%) events
299 occurred after a rainfall depth lower than 5 mm, 187 events (82%) took place in response to rainfall
300 depths higher than 5 mm, including 104 (47%) runoff events occurring following rainfall depths higher
301 than 10 mm (Figure 3).



302
303 Figure 3: Boxplots of a) rainfall depth that resulted in runoff events and b) corresponding runoff depth
304 (logarithmic scale in the y-axis).

305 Most runoff events (Figure 3b) occurred during autumn (49%) and winter (31%). Runoff events were
306 also recorded during summer (14%) and spring (6%). Interestingly, a significantly higher rainfall depth
307 was required to generate runoff event in summer than in winter: the corresponding median rainfall
308 depths amounted to 15 mm and 8.2 mm, respectively (Figure 3a), and the median runoff depth
309 amounted 0.05 mm and 0.1 mm, respectively (Figure 3b). In this case, runoff occurrence is related to
310 the high variability in infiltration capacity over seasons resulting from surface crusting, with infiltration
311 rates ranging from 2 mm.h⁻¹ to 50 mm.h⁻¹ (Cerdan et al., 2002a).

312 The evolution of crop types over the monitoring period is provided in Figure 4.



314 Figure 4: Crop type evolution during the monitoring period. Each year is corresponding to agricultural years,
 315 starting in September, e.g. “2008” is corresponding to 1st September 2007 to 31 August 2008. Intercrops were
 316 not included in this analysis. No data values corresponded to periods when it was not possible to collect data
 317 from landowners.

318 The cultivated areas were dominated by winter crops (60%), including wheat, rapeseed and winter
 319 barley. Spring crops, including flax, sugar beet, maize and potatoes, represented 35% of the cultivated
 320 area. These crops were also the most widely cultivated plants crops in Europe for the period 2009-
 321 2019, and including common wheat, maize and corn-cob mix, barley, oats and rye (Eurostat, 2019).
 322 The observed crops are therefore representative of the most commonly cultivated plants in Europe.

323 The current study took advantage of extensive field measurements obtained with the active
 324 cooperation of landowners. Consequently, a unique long-term monitoring of crop types and shallow
 325 tillage operations was available for this study. At large scales, such data are usually not available, but
 326 interesting approaches such as crop rotation simulations (Schönhart et al., 2011; Sietz et al., 2021) may
 327 contribute to improve such shortcomings. The proposed database from our study may be used to
 328 validate such approaches.

329 3.2. Crop cover evolution

330 Crop cover evolution was evaluated over the entire catchment based the soil surface state observation.

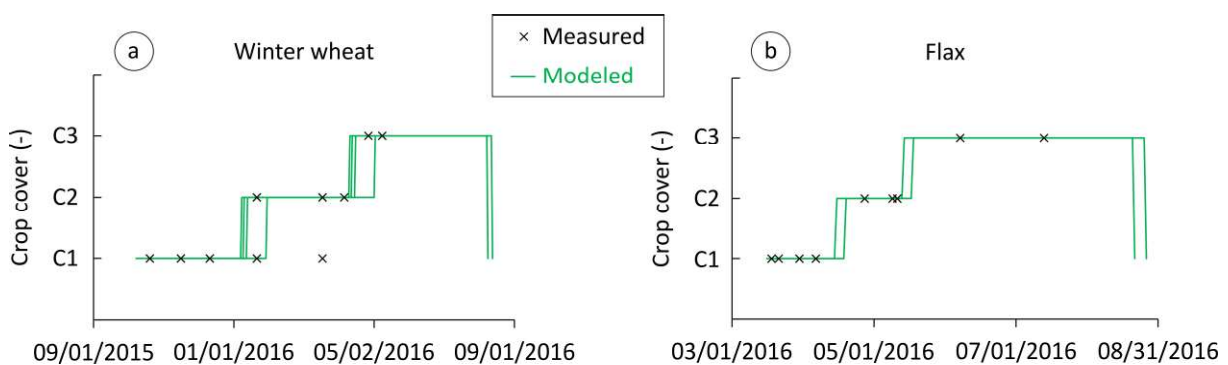
331 The mean seeding date corresponded to mean values obtained from the farmers' interviews. The

332 resulting crop cover evolution is proposed in Table 2.

Crop cover	Mean seeding date	20%	40%	60%	80%	100%
Crop cover class	(0 %)					
	C1	C2		C3		
Crop type	Crops growing (days)					
Sugar beets, cabbages, spinach	April 15 th	44	75	83	102	107
Maize	April 25 th	66	82	92	114	124
Flax, alfalfa	March 15 th	29	48	58	76	81
Peas, faba beans, beans	March 30 th	55	76	87	93	103
Potatoes	April 15 th	45	65	72	88	93
Oats, rye, radish	April 10 th	25	45	55	61	66
Wheat	October 20 th	92	136	186	193	203
Barley	October 5 th	77	154	176	198	208
Rapeseed	September 5 th	61	77	207	210	215
Ryegrass, clover	September 5 th	40	57	71	73	107
Intercrops with mustard	September 5 th	30	45	55	57	64
Intercrops with phacelia	September 1 st	39	54	64	72	82
Intercrops: mustard or faba bean		d+50	d+30	d+20	d+10	d
Intercrops: other types		d+50	d+35	d+25	d+15	d

333 Table 2 : Soil cover parameterization deduced from the field survey. Numbers indicate the days required to reach
 334 the corresponding crop cover. The “d” letter corresponded to crops destruction.

335 Crop cover was divided into 5 segments (0% to 100% in 20% increments) to allow for a smoother
 336 transition between classes, particularly for crusting and roughness evolutions (see section 3.3 below).
 337 However, they were aggregated in three classes (0%-20%; 21%-60%; 61%-100%) for comparison with
 338 measurements. After the progressive crop cover increase during the growing period, different
 339 operations were considered for explaining the crop cover decrease: chemical destruction, harvesting,
 340 mechanical destruction, and ploughing. Intercrop chemical destruction was estimated to result in a
 341 progressive decrease from a fully developed crop or intercrop to a limited cover in 50 days (Martin,
 342 1997). Conversely, harvesting and ploughing resulted in a quick decrease from a maximal to a limited
 343 crop cover. The initial crop cover of the following crop type was therefore defined based on the
 344 previous crop type and latest farming operation. An illustration of the modeled and observed crop
 345 covers for the two most common winter and spring crops is provided in Figure 5. For evaluation over
 346 other crop types and on the Blossenville catchment, additional figures were provided as supplementary
 347 material.



348 Figure 5: Measured (black crosses) and modeled (green continuous line) crop cover for the two most common
 349 crops observed in the catchment: a) winter wheat (four plots were monitored) and b) flax (two plots were
 350 monitored). The different lines corresponded to different modeled plots. The differences between lines is linked
 351 to differences in seeding dates.
 352

353 The modeled crop cover over the eight crop types detailed in Table 1 matched the observation for 73%
354 of the records, indicating a good parameterization performance. The agreement between modeled
355 and measured values was statistically significant. It should however be noticed that some temporal
356 variability was observed. For instance, the measured crop cover for winter wheat varied between C1
357 (0% - 20%) and C2 (21% - 60%) from 21st January to 18th March (Figure 5a), depending on the monitored
358 plots. It indicated some inherent variability in crop cover that was only partly explained by the
359 differences in seeding dates, reflected by the modeled variability between plots (e.g. maize;
360 supplementary material). Interestingly, the proposed values were in agreement with data collected in
361 the literature in various contexts. For instance, Tang et al. (2018) measured that the crop cover was
362 maximal for winter wheat approximately 180 days after sowing, while our measurements indicated a
363 corresponding period of approximately 190 days. Deng et al. (2012) indicated that the maximal plant
364 growth was measured after 90 days for flax and 140 days for maize, while we found in our study values
365 of 80 and 130 days, respectively. The agreement in ranges between the values proposed in this study
366 and the results reported in the literature suggest that the simple approach proposed in this study may
367 be applied to other catchments to obtain reliable although rough estimates of crop growing.

368 3.3. Soil crusting and roughness evolution

369 The initial values for roughness and surface crusting depend on the previous (inter-)crop type and crop
370 operation. For instance, ploughing results in a high surface roughness (i.e. > 10 cm), a value that may
371 also be observed for potato crops. Therefore, for each crop type, the initial surface roughness and
372 surface crusting were assumed to be controlled by the previous crop operation (e.g. ploughing,
373 mechanical destruction) and the current crop type. In addition to this temporal evolution, initial values
374 for crusting and roughness were therefore proposed and included as inputs for each crop type.

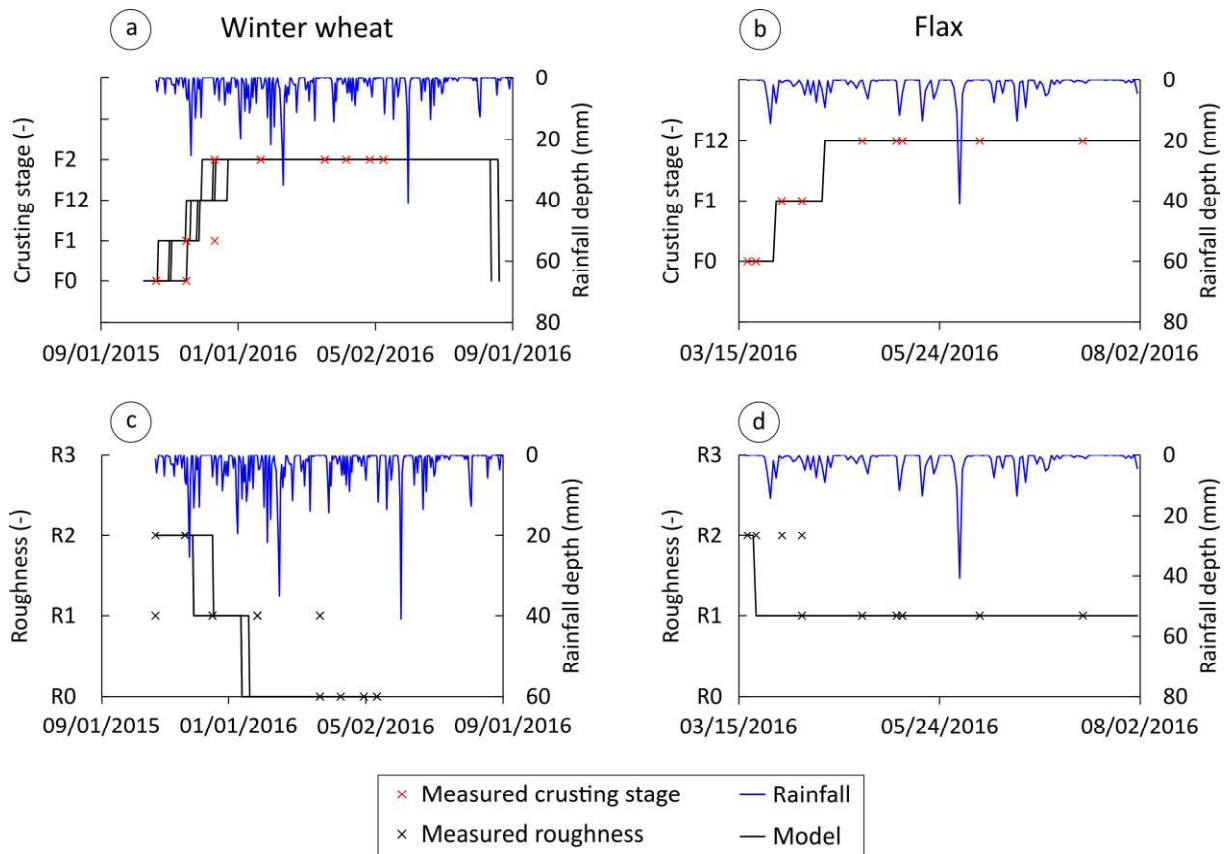
375 In this study, a parameterization of crusting and roughness evolution based on daily rainfall data
376 (Ndiaye et al., 2005; Vinci et al., 2020) was proposed, taking into account the protective effects of the
377 crop cover. Indeed, increasing the soil cover by vegetation was demonstrated to reduce the rainfall

378 kinetic energy (e.g. Brandt et al., 1989) and, therefore, the soil aggregate breakdown, limiting crusting
 379 and roughness decrease. The parameterization, including Table 2 and Table 3, was initially based on
 380 expert knowledge acquired in this region during the past decades (e.g. Auzet et al., 1990; Ouvry and
 381 Ligneau, 1993, Martin et al., 2010), and was then adapted using the measurements acquired during
 382 this study and collected from Delmas et al. (2012). The resulting parameterization is proposed in Table
 383 3 to define roughness and crusting evolution over time and rainfall for various crop covers (as defined
 384 in section 3.2).

Crop cover		0%-20%	20%-40%	40%-60%	60%-80%	80%-100%
	R4 → R3	150	190	225	300	375
Surface roughness	R3 → R2	120	150	180	240	300
	R2 → R1	120	150	180	240	300
	R1 → R0	120	150	180	240	300
Surface crusting	F0 → F1	30	45	90	115	120
	F1 → F12	35	50	100	125	130
	F12 → F2	90	130	265	335	350

385 Table 3: Soil roughness and crusting evolution under rainfall. The numbers indicate the rainfall depth (mm)
 386 required to reach the corresponding roughness or crusting stage, for each crop cover class (columns).

387 An illustration of the proposed parameterization and comparison with measurements for crusting
 388 stages and soil roughness is presented in Figure 6. Additional figures presented as supplementary
 389 material presented the parameterization results for other crop types.



390

391 Figure 6: Measured (crosses) and modeled (continuous line) crusting stage (a and b, red crosses) and soil
 392 roughness (c and d, black crosses) for winter wheat and flax. The continuous blue line represents daily rainfall.

393 The agreement between observed and modeled values reached 63% for the crusting stage and 74%
 394 for the roughness, and was statistically significant. The limited performance for crusting is partly
 395 explained by the poor performance obtained for fields cultivated with potatoes (22%, p-value=0.24).

396 This is related to the limited crop cover in the early stages of plant growth, the modeled crusting stage
 397 quickly increased to reach the stage of crusted soil with sedimentary crust (F2). However, crusting is
 398 assumed to remain limited on inter-rows, as reflected by measurements indicating the occurrence of
 399 a structural stage (F1) during 72% of the monitoring period, ranging from April to August for this crop
 400 type, and that of intermediate crusting (F12) as maximal observed crusting stage. Therefore, the
 401 parameterization performance remained low for this crop type. Consequently, crusting evolution for
 402 soil surface with high initial roughness (R4) should be considered with caution, and further
 403 developments should include a relationship between crusting and roughness.

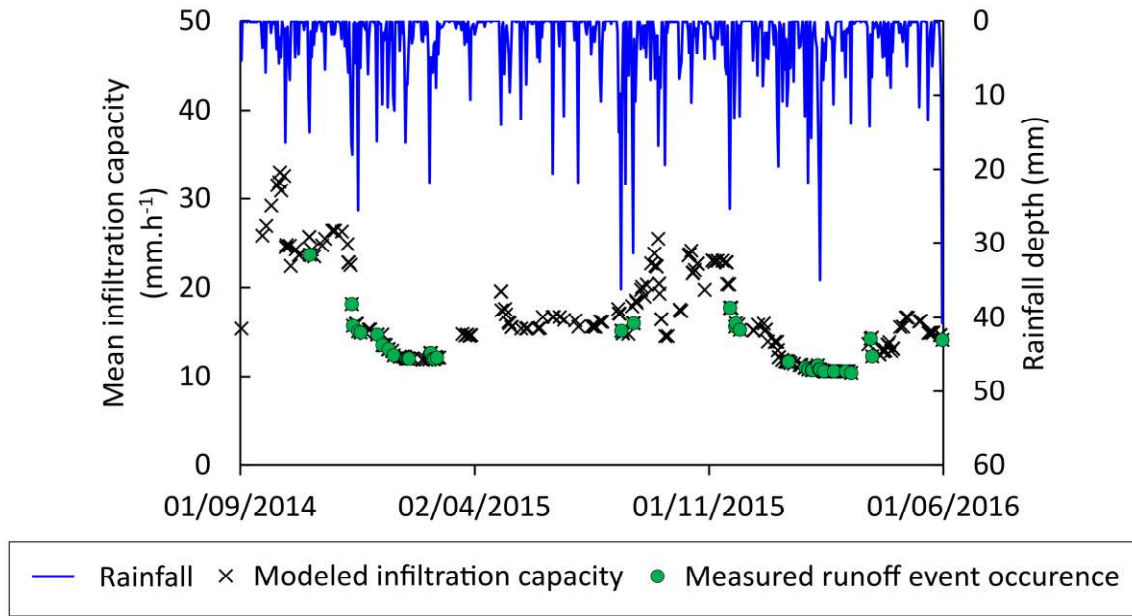
404 3.4. Evaluation of the parameterization extrapolation abilities

405 In addition to parameterization evaluation as performed in sections 3.2 and 3.3, we assessed whether
406 the PREMACHE framework could be applied to other catchments by using the 109 observations of the
407 Blosseville catchment. Results from the Blosseville catchments are presented in supplementary
408 material. For the 20 monitored plots covered with wheat (7 plots), flax (2 plots), peas (3 plots) and
409 winter barley (3 plots), the predicted crop cover was good. The modeled values corresponded to
410 measurements in 91% of the cases. Errors were observed regarding the occurrence of intermediate
411 crop cover (C2) on fields planted with peas and wheat. For crusting, only data for fields cultivated with
412 flax and peas were available, and the parameterization matched the observations in 87% of the cases,
413 with the few errors occurring regarding the prediction of the structural crusting stage (F1). Finally, for
414 roughness, the parameterization performance was acceptable, with 82% of agreement between
415 observations and modeled values, mainly due to errors to predict the roughness early stages for fields
416 planted with wheat and winter barley: after seeding (occurring the 8th October) the observations
417 indicated a limited roughness (R1) while the parameterization predicted a slightly higher roughness
418 (R2) until mid-December. However, given the variations observed in the measurements, the model
419 performance could be considered as acceptable.

420 3.5. Implications for runoff modelling

421 Adequately representing the variability of soil hydrodynamic properties, such as infiltration capacity,
422 is a long-standing issue for runoff modelers. Moreover, in agricultural catchments, the significance of
423 shallow tillage operations can dramatically change these properties within a very short period of time
424 (Martin et al., 2004). The PREMACHE software proposes an alternative method to account for these
425 variations in runoff modelling, which may be crucial in understanding catchments hydrological
426 behavior (Wagner et al., 2019). As an illustrative example of the approach, the Bourville catchment
427 mean infiltration capacity was modeled over two entire crop cycles. Calculations were performed from
428 1st September 2014 to 1st September 2016. For readability purpose, results are presented for 1st
429 September 2014 to 1st June 2016, corresponding to a total of 253 rainfall events, as no significant runoff

430 event was recorded after 1st June 2016. For each of these rainfall events, the mean infiltration capacity,
 431 weighted by the plot surface, was reported. The link between infiltration capacity and runoff was
 432 visually suggested by indicating periods when runoff events were measured at the catchment outlet
 433 (Figure 7).



434
 435 Figure 7: Modeled mean weighted infiltration capacity (black crosses) for each measured rainfall event and daily
 436 rainfall (blue continuous line) in the Bourville catchment. Green circles indicate when rainfall events generated
 437 a runoff event that was measured at the catchment outlet.

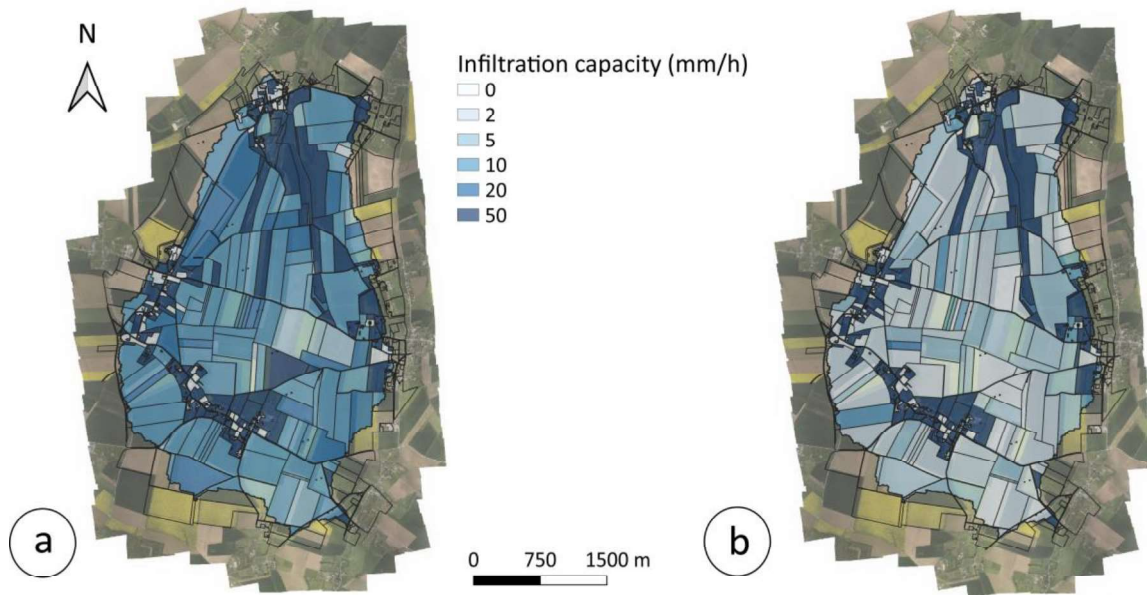
438 This result illustrated the dynamics of soil infiltration capacity and its impact on the catchment runoff
 439 dynamics. From November 2014 to February 2015, 41 rainfall events with a rainfall depth higher than
 440 1 mm were recorded over 92 days. Consequently, soil crusting progressively increased, resulting in a
 441 decreased infiltration capacity, from 33 mm.h⁻¹ to 12 mm.h⁻¹, with direct implications for runoff
 442 generation (Ndiaye et al., 2005). This decrease occurred mainly because of three major storm events
 443 accumulating 60.2 mm. On some cultivated fields, infiltration capacity dropped from 50 mm.h⁻¹ in
 444 November 2014 to 2 mm.h⁻¹ in February 2015. This indicated that the soils were crusted with the
 445 occurrence of a sedimentary crust, resulting in a very limited infiltration capacity. After harvesting and
 446 spring crops seeding, crop cover decreased and crusting removal through shallow tillage operations

447 resulted in an increased infiltration capacity, up to 26 mm.h⁻¹ (November 2015). This increase
448 underlined the importance of shallow tillage operations in controlling the infiltration rates of the
449 catchment and, more generally, on soil properties (Strudley et al., 2008). Future developments may
450 include the effects of the tillage type (Osunbitan et al., 2005) and long-term farming methods (Basche
451 and DeLonge, 2019).

452 Then, an unusually wet period occurred in September 2015 resulted in widespread soil crusting. The
453 mean infiltration capacity decreased again to 15 mm.h⁻¹. Rainfall depth was 87.8 mm in September
454 2015 while the measured mean was 56 mm. Shallow tillage operations performed across multiple
455 fields had a strong influence on the catchment-scale infiltration capacity (Martin et al., 2010). It
456 increased soil infiltration capacity to 24 mm.h⁻¹ in October 2015, followed by another progressive
457 decrease during winter. This high-frequency result indicated that the soils' hydrodynamics might
458 exhibit quick variations due to the combination of rainfall and tillage operations and may be taken into
459 account with the simple parameterization proposed in the current research.

460 Interestingly, this result illustrates the dominance of infiltration-excess runoff. Runoff events, as
461 defined in section 2.3 (i.e. based on a threshold on runoff volume and discharge peak), occurred mainly
462 when rainfall increased crusting, resulting in a mean infiltration capacity below 20 mm.h⁻¹. The
463 PREMACHE software may therefore be used to provide inputs for runoff and erosion models and to
464 increase their performance by taking into account the fast (e.g. progressive crusting in winter and
465 tillage operations) and long-term (cycles over multiple years) dynamics of soil infiltration capacity. It
466 therefore offers a possibility to quantify the infiltration-runoff partition and could therefore
467 complement existing modelling approaches such as that including curve number variations in models
468 (Mehdi et al., 2015). This may be useful in agricultural catchments, as both infiltration-excess and
469 saturation-excess may be involved in generating flood events in such environments (Saffarpour et al.,
470 2016; Grangeon et al., 2021).

471 In addition to the temporal dynamics, it is also important to consider the spatial variations of
472 infiltration capacity at the catchment scale (Figure 8).



473
474 Figure 8: Spatial distribution of infiltration capacity in the Bourville catchment, as simulated by the PREMACHE
475 software in a) November 2015 (mean infiltration capacity: 33 mm.h⁻¹) and b) February 2016 (mean infiltration
476 capacity: 12 mm.h⁻¹).

477 Plot-to-plot variations was mainly related to differences in crop types and soil surface states. These
478 spatial variations have important implications for runoff triggering. In particular, grasslands,
479 characterized by a high infiltration capacity (in this study, 50 mm.h⁻¹), were located in a talweg in the
480 northern part of the Bourville catchment, concentrating runoff at locations with a high infiltration
481 capacity. It will therefore decrease runoff volumes recorded at the outlet regardless the considered
482 season. Depending on the considered rainfall events, it might affect the areas producing runoff and
483 those infiltrating the runoff volumes, therefore affecting the hydrological connectivity (Darboux et al.,
484 2001), which was previously demonstrated to be affected by landscape patchiness (e.g. Baartman et
485 al., 2020). Of note, specific cases such as the effects of grazing on pastures infiltration capacity
486 (Joannon, 2004) were not included in this analysis. However, they can be accounted for by creating a
487 dedicated field in the toolbox.

488 The current study proposed an approach to account for spatiotemporal variations in soil hydrodynamic
489 properties in complex catchments including agricultural areas. Based on simple inputs, it is
490 complementary to existing modelling approaches in that it can also incorporate other knowledge or
491 model inputs.

492 4. Conclusions

493 In the current research, existing knowledge on soil surface state and a unique database were compiled.
494 The database included the monitoring of crop types and soil surface state, as well as the high-
495 resolution measurement of rainfall and runoff. Although the monitored sites corresponded to loamy
496 soils sensitive to surface crusting under temperate climatic conditions, they may be representative of
497 the conditions observed in other cultivated regions where hydrological processes are dominated by
498 infiltration-excess runoff.

499 A framework describing the soil surface state dynamics was developed and included in a software
500 made available for download. It made use of limited field data inputs: crop types and tillage operations
501 at different observation dates, and rainfall time series. It was demonstrated to adequately reproduce
502 the changes in crop cover, soil crusting and roughness on various crop types, in two different
503 catchments. Previous research results were used to convert these soil surface states into
504 hydrodynamic properties such as infiltration capacity. The software used in this study was made
505 available for download and can be used to support runoff modelling in agricultural catchments where
506 experimental data are lacking, using either the proposed default values or modifications based on
507 modeler's knowledge.

508 When applied to the studied catchment, results demonstrated the high variability of soil infiltration
509 capacity between crop types, depending on the sequences of tillage operations and rainfall dynamics.
510 The variations in infiltration capacity at the catchment scale and for various time scales, from the
511 rainfall event to the inter-annual scale, and its strong implications for runoff modelling were illustrated.
512 The proposed approach allows representing this variability in runoff models by creating runoff model

513 inputs, based on a large database proposed along with the manuscript. It may therefore be useful for
514 applications in unmonitored agricultural areas in general and more specifically on loamy soils,
515 susceptible to crusting. It will help representing the temporal and spatial variability of soils
516 hydrodynamic properties for different crops and a sequence of hydrological years, which will
517 ultimately contribute to a better understanding of runoff pathways and hydrological connectivity at
518 the catchment scale.

519 **Acknowledgments:** The general idea of this manuscript, based on soil surface state, largely originated
520 from the pioneering work of late Yves Le Bissonnais. We would particularly like to thank the
521 landowners for their involvement in the data collection and for granting access to their fields, making
522 this long-term work possible: Mrs. Baret, Bazire, Bouclon, Burel, Cabot, Constantin, Cordier,
523 Delafontaine, Delamare, Delaunay, Grindel, Laguerre, Larcher, Lefrançois, Martine, Mignot, Moonen
524 van Meer, Olivier, Pesqueux, Petit, Planchon, Poulet, Rossignol, Roussel, Terrier and Voisin. The
525 assistance of Mathieu Saulnier in field measurements is acknowledged. Thomas Grangeon would like
526 to thank Farid Smai and Theophile Guillon for their help in model formatting and GitHub deposit. The
527 two anonymous reviewers provided constructive and detailed comments that helped improving the
528 manuscript quality.

529 **Funding:** The monitoring of the Bourville catchment was supported by the Seine Normandy Water
530 Agency within the framework of the Pesticeros project.

531 This work has been supported by the French State financial support managed by the Agence Nationale
532 de la Recherche, allocated in the “Investissements d’Avenir” framework programme under reference
533 ANR-11-RSNR-0002 (AMORAD project).

534 **Author contributions:** JFO initiated the data acquisition on the Bourville catchment and secured the
535 essential, yet uncommon, long-term funding needed to acquire representative measurements. JFO,
536 LTP and JBR performed the crop observations, soil surface state measurements and farmers’
537 interviews. PM and OC provided additional experimental data for model calibration and validation.
538 JFO, OC and JBR created the model parameterization, further modified by TG, RV and OC. TG, RV and
539 LTP processed the rainfall and runoff data. RV wrote the first model version, further modified by TG.
540 TG wrote the manuscript. All co-authors commented the manuscript.

541 **Software and data availability:** The data used in this study (Excel spreadsheets and shapefiles) and the
542 PREMACHE toolbox are available at <https://github.com/BRGM/premache>.

543 PREMACHE is licensed under GPL V3.0. It was developed by Rosalie Vandromme and Thomas Grangeon
544 (r.vandromme@brgm.fr and t.grangeon@brgm.fr) in early 2021 under Python 3.8.5, using Windows
545 10, a 2.5 GHz i5-7300HQ CPU with 16 Go memory. Using this configuration, the model processed the
546 dataset proposed with the manuscript (a shapefile including approximately 1200 polygons monitored
547 over 9 years) and exported rasters at a 5 m resolution for a subset of 50 rainfall events in approximately
548 15 minutes.

549 References

- 550 Arnold J. G., Srinivasan R., Muttiah R.S., Williams J. R. (1998). Large area hydrologic modeling and
551 assessment—Part 1: Model development. *Journal of the American Water Resources Association*,
552 **34(1)**:73-89.
- 553 Assouline S., Mualem Y. (1997). Modeling the dynamics of seal formation and its effect on infiltration
554 as related to soil and rainfall characteristics. *Water Resources Research*, **33(7)**:1527-1536.
- 555 Auzet A.V., Boiffin J., Papy F., Maucorps J., Ouvry J.F. (1990). An approach to the assessment of erosion
556 forms and erosion risk on agricultural land in the northern Paris Basin, France. In: Boardman J., Foster
557 I.D.L., Dearing J.A. (Eds.), *Soil Erosion on Agricultural Land*. Wiley, Chichester, UK, pp. 383–400
- 558 Auzet A.V., Boiffin J., Papy F., Ludwig B., Maucorps J. (1993). Rill erosion as a function of the
559 characteristics of cultivated catchments in the North of France. *Catena*, **20**:41-62.
- 560 Auzet A.V., Boiffin J., Ludwig B. (1995). Concentrated flow erosion in cultivated catchments: influence
561 of soil surface state. *Earth Surface Processes and Landforms*, **20(8)**:759-767.
- 562 Baartman J.E.L., Nunes J.P., Masselink R., Darboux F., Biielders C., Degré A., Cantreul V., Cerdan O.,
563 Grangeon T., Fiener P., Wilken F., Schindewolf M., Wainwright J. (2020). What do models tell us about
564 water and sediment connectivity? *Geomorphology*, **367**:107300.
- 565 Basche A.D., DeLonge M.S. (2019). Comparing infiltration rates in soils managed with conventional and
566 alternative farming methods: A meta-analysis. *PLoS ONE*, **14(9)**:e0215702.
- 567 Baumhardt R.L., Romkens M.J.M., Parlange J.Y., Whisler F.D. (1991). Predicting soil-surface seal
568 conductance from incipient ponding and infiltration data. *Journal of Hydrology*, **128(1-4)**:277-291.
- 569 Ballabio C., Panagos P., Montanarella L. (2016). Mapping topsoil physical properties at European scale
570 using the LUCAS database. *Geoderma*, **261**:110-123.

571 Bieger K., Arnold J.G., Rathjens H., White M.J., Bosch D.D., Allen P.M., Volk M., Srinivasan R. (2017).
572 Introduction to SWAT+, a completely restructures version of the Soil and Water Assessment Tool.
573 *Journal of the American Water Resources Association*, **53(1)**:115-130.

574 Boardman, J., Ligneau, L., de Roo, A., Vandaele, K., (1994). Flooding of property by runoff from
575 agricultural land in northwestern Europe. *Geomorphology*, **10**:183–196.

576 Boardman, J. (2010). A short history of muddy floods. *Land Degradation & Development*, **21**:303-309.

577 Boardman J. (2020). A 38-year record of muddy flooding at Breaky Bottom: Learning from a detailed
578 case study. *Catena*, **189**:104493.

579 Boas T., Bogena H., Grünwald T., Heinesch B., Ryu D., Schmidt M., Vereecken H., Western A., Franssen
580 H.J.H. (2021). Improving the representation of cropland sites in the Community Land Model (CLM)
581 version 5.0. *Geoscientific Model Development*, **14**:573-601.

582 Boiffin J., Papy F., Eimberck M. (1988). Influence des systèmes de culture sur les risques d'érosion par
583 ruissellement concentré : I. Analyse des conditions de déclenchement de l'érosion. *Agronomie* **8**:663–
584 673.

585 Brakensiek D.L., Rawls W.A. (1983). Agricultural management effects on soil water processes. Part II.
586 Green and Ampt parameters for crusting soils. *Transactions of the ASAE*, **26(6)**:1753 1757

587 Brandt C.J. (1989). The size distribution of throughfall drops under vegetation canopies. *Catena*
588 **16**:507–524.

589 Bresson L.M., Boiffin J. (1990). Morphological characterisation of soil crust development stages on an
590 experimental field. *Geoderma*, **47**:301–325.

591 Casenave A., Valentin C. (1992). A runoff capability classification-system based on surface-features
592 criteria in semiarid areas of West Africa. *Journal of Hydrology*, **130(1-4)**:231-249.

593 Cerdan O., Souchère V., Leconte V., Couturier A., Le Bissonnais Y. (2002a). Incorporating soil surface
594 crusting processes in an expert-based runoff model: Sealing and Transfer by Runoff and Erosion related
595 to Agricultural Management. *Catena*, **46**:189-205.

596 Cerdan O., Le Bissonnais Y., Couturier A., Saby N. (2002b). Modelling interrill erosion in small cultivated
597 catchments. *Hydrological Processes*, **16**:3215-3226.

598 Cerdan O., Le Bissonnais Y., Govers G., Lecomte V., van Oost K., Couturier A., King C., Dubreuil N. (2004).
599 Scale effect on runoff from experimental plots to catchments in agricultural areas in Normandy. *Journal*
600 *of Hydrology*, **299(1-2)**:4-14.

601 Darboux F., Davy P., Gascuel-Oudou C., Huang C. (2001). Evolution of soil surface roughness and
602 flowpath connectivity in overland flow experiments. *Catena*, **46**:125-139.

603 Delmas M., Pak L.T., Cerdan O., Souchère V., Le Bissonnais Y., Couturier A., Sorel L. (2012). Erosion and
604 sediment budget across scale: A case study in a catchment of European loess belt. *Journal of Hydrology*,
605 **420-421**:255-263.

606 De Roo A.P.J., Riezebos H.T. (1992). Infiltration experiments on loess soils and their implications for
607 modeling surface runoff and soil erosion. *Catena*, **19(2)**:221-239.

608 De Roo A.P.J., Wesseling C.G., Ritsema C.J. (1996). LISEM: a single-event, physically based hydrological
609 and soil erosion model for drainage basins. I: Theory, input and output. *Hydrological Processes*, **10**:
610 1107-1117.

611 Deng J., Ran J., Wang Z., Fan Z., Wang G., Ji M., Liu J., Wang Y., Liu J., Brown J.H. (2012). Models and
612 tests of optimal density and maximal yield for crop plants. *PNAS*, **109(39)**:15823-15828.

613 Duley F.L. (1939). Surface factors affecting the rate of intake of water by soils. *Soil Science Society of*
614 *America Proceedings*, **4**:60-64.

615 Eghbal M.K., Hajabbasi M.A., Golesefidi H.T. (1996). Mechanism of crust formation on a soil in central
616 Iran. *Plant and Soil*, **180(1)**:67-73.

617 Eldrige D.J., Zaady E., Shachak M. (2000). Infiltration through three contrasting biological soil crusts
618 in patterned landscapes in the Negev, Israel. *Catena*, **40(3)**:323-336.

619 Eurostat (2019). Production of main cereals, EU-27, 2009-2019.
620 [https://ec.europa.eu/eurostat/statistics-](https://ec.europa.eu/eurostat/statistics-explained/index.php?title=File:Production_of_main_cereals,_EU-27,_2009-2019_(million_tonnes)_AFF2020.png)
621 [explained/index.php?title=File:Production_of_main_cereals,_EU-27,_2009-](https://ec.europa.eu/eurostat/statistics-explained/index.php?title=File:Production_of_main_cereals,_EU-27,_2009-2019_(million_tonnes)_AFF2020.png)
622 [2019_\(million_tonnes\)_AFF2020.png](https://ec.europa.eu/eurostat/statistics-explained/index.php?title=File:Production_of_main_cereals,_EU-27,_2009-2019_(million_tonnes)_AFF2020.png). Last access: 24th March 2022.

623 Evrard, O., Bièlders, C.L., Vandaele, K., van Wesemael, B. (2007). Spatial and temporal variation of
624 muddy floods in central Belgium, off-site impacts and potential control measures. *Catena*, **70**:443-454.

625 Evrard, O., Vandaele, K., Bièlders, C., Wesemael, B. (2008). Seasonal evolution of runoff generation on
626 agricultural land in the Belgian loess belt and implications for muddy flood triggering. *Earth Surface*
627 *Processes and Landforms*, **33**:1285-1301.

628 Evrard O., Cerdan O., van Wesemael B., Chauvet M., Le Bissonnais Y., Raclot D., Vandaele K., Andrieux
629 P., Bièlders C. (2009). Reliability of an expert-based runoff and erosion model: Application of STREAM
630 to different environments. *Catena*, **78(2)**:129-141.

631 Evrard, O., Heitz, C., Liègeois, M., Boardman, J., Vandaele, K., Auzet, A.V., van Wesemael, B. (2010). A
632 comparison of management approaches to control muddy floods in central Belgium, northern France
633 and southern England. *Land Degradation & Development*, **21**:322-335.

634 Foley J.L., Loch R.J., Glanville S.F., Connolly R.D. (1991). Effects of tillage, stubble and rainfall energy on
635 infiltration. *Soil and Tillage Research*, **20(1)**:45-55.

636 Garen D.C., Moore D.S. (2005). Curve number hydrology in water quality modeling: Uses, abuses and
637 future directions. *Journal of the American Water Resources Association*, **41(2)**:377-388.

638 Gascuel-Oudoux C., Arousseau P., Cordier M.O., Durand P., Garcia F., Masson V., Salmon-Monviola J.,
639 Tortrat F., Trepos R. (2009). A decision-oriented model to evaluate the effect of land use and
640 agricultural management on herbicide contamination in stream water. *Environmental Modelling and*
641 *Software*, **24**:1433-1446.

642 Gascuel-Oudoux C., Arousseau P., Doray T., Squidant H., Macary F., Uny D., Grimaldi C. (2011).
643 Incorporating landscape features to obtain an object-oriented landscape drainage network
644 representing the connectivity of surface flow pathways over rural catchments. *Hydrological Processes*,
645 **25**:3625-3636.

646 Gilley J.E., Kottwitz E.R., Wieman G. (1991). Roughness Coefficients for Selected Residue Materials.
647 *Journal of Irrigation and Drainage Engineering*, **117**:503–514.

648 Grangeon T., Ceriani V., Evrard O., Grison A., Vandromme R., Gaillot A., Cerdan O., Salvador-Blanes S.
649 (2021). Quantifying hydro-sedimentary transfers in a lowland tile-drained agricultural catchment.
650 *Catena*, **198**:105033.

651 Gumiere S.J., Raclot D., Cheviron B., Davy G., Louchart X., Fabre J.C., Moussa R., Le Bissonnais Y. (2011).
652 MHYDAS-Erosion: a distributed single-storm water erosion model for agricultural catchments.
653 *Hydrological Processes*, **25**:1717-1728.

654 Hawkins R.H. (2014). Curve number method: Time to think anew ? *Journal of Hydrologic Engineering*,
655 **19**(6). DOI: 10.1061/(ASCE)HE.1943-5584.0000954.

656 Joannon A. (2004). Spatial coordination of cropping systems to control ecological processes. Case study
657 of runoff in agricultural catchment basins of the Pays de Caux, France. PhD Thesis, 393 pp. INAPG
658 (AgroParisTech). NNT :2004INAP0018. Pastel-00001257.

659 King, D., Le Bissonnais, Y., (1992). Rôle des sols et des pratiques culturales dans l'infiltration et
660 l'écoulement des eaux. Exemple du ruissellement et de l'érosion sur les plateaux limoneux du nord de
661 l'Europe. *Comptes Rendus de l'Academie d'Agriculture de France*, **78**(6): 91–105.

662 King K.W., Arnold J.G., Bingner R.I. (1999). Comparison of Green-Ampt and curve number methods on
663 Goodwin Creek watershed using SWAT. *Transaction of the ASAE*, **42(4)**:919-925.

664 Le Bissonnais Y., Singer M.J. (1992). Crusting, runoff, and erosion response to soil-water content and
665 successive rainfalls. *Soil Science Society of America Journal*, **56(6)**:1898-1903.

666 Le Bissonnais Y., Benkhadra H., Chaplot V., Fox D., King D., Daroussin J. (1998). Crusting, runoff and
667 sheet erosion on silty loamy soils at various scales and upscaling from m² to small catchments. *Soil &*
668 *Tillage Research*, **46**:69-80.

669 Le Bissonnais Y., Cerdan O., Lecomte V., Benkhadra H., Souchère V., Martin P. (2005). Variability of soil
670 surface characteristics influencing runoff and interrill erosion. *Catena*, **62**: 111–124.

671 Ludwig B. (1992). L'érosion par ruissellement concentre des terres cultivées du nord du bassin parisien
672 : analyse de la variabilité des symptômes d'érosion à l'échelle du bassin versant élémentaire. PhD
673 Thesis, *University of Strasbourg*, 201 pp.

674 Martin P. (1997). Pratiques culturales, ruissellement et érosion diffuse sur les plateau limoneux du
675 nord ouest de l'Europe. Application aux intercultures du Pays de Caux. PhD Thesis, *INA-PG*, 261 pp.

676 Martin P., Joannon A., Souchère V., Papy F. (2004). Management of soil surface characteristics for soil
677 and water conservation : The case of a silty loam region (Pays de Caux, France). *Earth Surface Processes*
678 *and Landforms*, **29**:1105-1115.

679 Martin P., Ouvry J.F., Bockstaller C. (2009). Application of the curve number approach to runoff
680 estimation for loamy soils over a growing season for winter wheat: Comparison with the STREAM
681 approach. *Land Degradation and Development*, **21**:376-387.

682 Martin P., Joannon A., Piskiewicz N. (2010). Temporal variability of surface runoff due to cropping
683 systems in cultivated catchment areas: Use of the DIAR model for the assessment of environmental
684 public policies in the Pays de Caux (France). *Journal of Environmental Management*, **91**:869-878.

685 Mehdi B., Ludwig R., Lehner B. (2015). Evaluating the impacts of climate change and crop land use
686 change on streamflow, nitrated and phosphorous: A modeling study in Bavaria. *Journal of Hydrology:
687 Regional Studies*, **4**:60-90.

688 Morgan R.P.C. (2005). Soil erosion and conservation. Third edition, Blackwell Publishing.

689 Moss A.J., Watson C.L. (1991). Rain-impacted soil crust. 3. Effects of continuous and flawed crusts on
690 infiltration, and the ability of plant covers to maintain crustal flaws. *Australian Journal of Soil Research*,
691 **29(2)**:311-330.

692 Msigwa A., Chawanda C.J., Komakech H.C., Nkwasa A., Van Griensven A. (under review) Representation
693 of seasonal land-use dynamics in SWAT+ for improved assessment of blue and green water
694 consumption. *Hydrology and Earth Systems Sciences*. [https://hess.copernicus.org/preprints/hess-
695 2021-171/](https://hess.copernicus.org/preprints/hess-2021-171/). Last access: 24th March 2022.

696 Ndiaye B., Esteves M., Vandervaere J.P., Lapetite J.M., Vauclin M. (2005). Effect of rainfall and tillage
697 direction on the evolution of surface crusts, soil hydraulic properties and runoff generation for a sandy
698 loam soil. *Journal of Hydrology*, **307**:294-311.

699 Nkwasa A., Chawanda C.J., Msigwa A., Komakech H.C., Verbeiren B., Van Griensven A. (2020). How can
700 we represent seasonal land use dynamics in SWAT and SWAT+ models for African cultivated
701 catchments? *Water*, **12**,1541. DOI: 10.3390/w12061541.

702 Osunbitan J.A., Oyedele D.J., Adekalu K.O. (2005). Tillage effects on bulk density, hydraulic conductivity
703 and strength of a loamy sand soil in southwestern Nigeria. *Soil and Tillage Research*, **82(1)**:57-64.

704 Ouvry J.F., Ligneau L. (1993). A specific strategy set-up with farmers to succeed erosion control – The
705 experience of a French region Pays de Caux. In: Wicherek S., *Farm land erosion in temperate plains
706 environments and hills*, pp. 497-502.

707 Owens P.N., Batalla R.J., Collins A.J., Gomez B., Hicks D.M., Horowitz A.J., Kondolf G.M., Marden
708 M., Page M.J., Peacock D.H., Petticrew E.L., Salomons W., Trustrum N.A. (2005). Fine-

709 grained sediment in river systems: environmental significance and management issues. *River*
710 *research and applications*, **21**: 693–717.

711 Peñuela A., Sellami H., Smith H.G. (2018). A model for catchment soil erosion management in humid
712 agricultural environments. *Earth Surface Processes and Landforms*, **43**:608-622.

713 Ponce V.M., Hawkins R.H. (1996). Runoff curve number: has it reached maturity? *Journal of Hydrologic*
714 *Engineering*, **1(1)**:11-19.

715 QGIS (2022). QGIS Geographic Information System. QGIS Association. <http://www.qgis.org>

716 Qi J., Lee S., Zhang X. Yang Q., Mc Carty G.W., Moglen G.E. (2020). Effects of surface runoff and
717 infiltration partition methods on hydrological modeling: A comparison of four schemes in two
718 watersheds in the Northeastern US. *Journal of Hydrology*, **581**:124415.

719 Richet J.B., Ouvry J.F., Pak L.T. (2021) Quantification des ruissellements pour les petits bassins versants
720 limoneux et karstiques de Normandie. Société Hydrotechnique de France, 35-49. ISBN 979-10-93567-
721 24-2. Available at: [https://bassinversant.org/wp-content/uploads/2021/02/Actes-](https://bassinversant.org/wp-content/uploads/2021/02/Actes-ruissellement_compressed.pdf)
722 [ruissellement_compressed.pdf](https://bassinversant.org/wp-content/uploads/2021/02/Actes-ruissellement_compressed.pdf). Last access: 24th March 2022.

723 Saffarpour S., Western A., Adams R., McDonnell J.J. (2016). Multiple runoff processes and multiple
724 thresholds control agricultural runoff generation. *Hydrology and Earth System Sciences*, **20**:4525-4545.

725 Schönhart M., Schmid E., Schneider U.A. (2011). CropRota – A crop rotation model to support
726 integrated land use assessments. *European Journal of Agronomy*, **34**:263-277.

727 Seginer I., Morin J. (1969). The effect of drop impact on the infiltration capacity of bare soils. Israel
728 Institute of Technology, Department of Agricultural Engineering, Publication No. 62. 16p.

729 Shore M., Murphy P.N.C., Jordan P., Mellander P.E., Kelly-Quinn M., Cushen M., Mechan S., Shine O.,
730 Melland A.R. (2013). Evaluation of a surface hydrological connectivity index in agricultural catchments.
731 *Environmental Modelling and Software*, **47**:7-15.

732 Sietz D., Conradt T., Krysanova V., Hatterman F.F., Wechsung F. (2021). The Crop Generator:
733 Implementing crop rotations to effectively advance eco-hydrological modelling. *Agricultural Systems*,
734 2021:103183. DOI: 10.1016/j.agsy.2021.103183.

735 Strudley M.W., Green T.R., Ascough II J.C. (2008). Tillage effects on soil hydraulic properties in space
736 and time: State of the science. *Soil and Tillage Research*, **99**:4-48.

737 Tang X., Song N., Chen Z., Wang J., He J. (2018). Estimating the potential yield and ET_c of winter wheat
738 across Huang-Huai-Hai Plain in the future with the modified DSSAT model, *Scientific Reports*, **8**:15370.

739 Valentin C. (1991). Surface crusting in two alluvial soils of northern Niger, *Geoderma*, **48**:201-222.

740 Van Dijk P.M., Kwaad F.J.P.M. (1996). Runoff generation and soil erosion in small agricultural
741 catchments with loess-derived soils. *Hydrological Processes*, **10(8)**:1049-1059.

742 Vinci A., Todisco F., Vergni L., Torri D. (2020). A comparative evaluation of random roughness indices
743 by rainfall simulator and photogrammetry. *Catena*, **188**:104468.

744 Wagner P.D., Bhallamudi S.M., Narasimhan B., Kumar S., Fohrer N., Fiener P. (2019). Comparing the
745 effects of dynamic versus static representation of land use change in hydrologic impacts assessments.
746 *Environmental Modelling and Software*, **122**:103987.